Mechanism and Machine Theory 121 (2018) 116–127

Contents lists available at ScienceDirect

Mechanism and Machine Theory

journal homepage: www.elsevier.com/locate/mechmachtheory

Research paper

Direct analysis of power-split CVTs: A unified method

Dario Rotella, Marco Cammalleri*

Dipartimento dell' Innovazione Industriale e Digitale, Università di Palermo, Italy

ARTICLE INFO

Article history:
Received 20 July 2017
Revised 20 September 2017
Accepted 8 October 2017

Keywords:
Continuously variable transmission
Power-split CVTs
Direct analysis
E-CVT
Hybrid
GM Voltec

ABSTRACT

This paper provides a fast kinematic analysis method for compound power-split CVTs, which consents to identify their functional parameters. Such parameters permit the assessment of power flows, torques and efficiency, and the design of equivalent transmissions by the use of a recently published mathematical model. The same method can easily address either simpler or more complex transmissions by mean of kinematic equivalent parameters, without the need to arrange separate systems of equations. As a case study, we performed the kinematic analysis of the "Voltec" multi-mode GM transmission.

1. Introduction

A new mathematical model for the preliminary design of power-split CVTs has been recently published [1]. It has been shown that a small number of functional parameters rule the operation of any power-split transmission: kinematics, power flows and efficiency can be assessed regardless the actual constructive layout.

In particular, these parameters govern a set of characteristic functions whose graphical representation, named *design-chart*, permits a quick comparison between the main features of different solutions, and can lead to important constructive simplifications, while taking efficiency-oriented choices.

Accordingly, for given target functional parameters, the method [1] leads the designer to choose a specific preliminary constructive concept, among all the possible solutions with one or two planetary gear trains and up to six ordinary gears.

However, despite the method [1] aims to the constructive feasibility of the involved gear sets, for instance it may be difficult to realize exactly the required ratios by means of concrete structures, because actual gear ratios are discrete. Therefore, a quick analysis method is necessary in order to assess the impact of a small variation of the constructive parameters on the transmission functioning, thus obtaining, for the chosen constructive scheme, its actual functional parameters.

This task is conceptually easy, and there are countless examples of similar analysis in literature [2–22]; nevertheless, none seems to provide a reasonably simple unified method in order to address all the possible different constructive solutions, especially when several functioning modes are involved. Accordingly, the main purpose of this article is to provide a unified method for the analysis of such transmissions, by identifying the functional parameters defined in [1].

Therefore, the method presented in this paper can be used to verify how much the target functional parameters will differ from the obtainable ones, but it also permits to analyze the operation of an existing power-split transmission as well

* Corresponding author.
E-mail addresses: dario.rotella@unipa.it (D. Rotella), marco.cammalleri@unipa.it (M. Cammalleri).

https://doi.org/10.1016/j.mechmachtheory.2017.10.006
0094-114X/

Nomenclature

An over-lined power or torque symbol refers to real working conditions

A	overall ratio spread
A_j	ratio spread of the jth shaft
i	input of the CVU
j	jth shaft
IN	input of the transmission
o	output of the CVU
OUT	output of the transmission
k_x	fixed speed ratio on the xth shaft of a three port differential
P_j	ideal power transmitted by the jth shaft
p_j	dimensionless ideal power transmitted by the jth shaft
p_i	dimensionless ideal power transmitted by the CVU
T_j	ideal torque applied to the jth shaft
α_j	implicit functional parameter
η	apparent efficiency of the PS-CVT
η_v	apparent efficiency of the CVU
τ	overall speed ratio (ω_{OUT}/ω_{IN})
τ'	normalized overall speed ratio (τ/τ_m)
τ_j	jth speed ratio (ω_j/ω_{IN})
τ_*	overall speed ratio concurrent with the synchronism of one planetary gear train
τ_v	CVU speed ratio (ω_o/ω_i)
$\tau_{\#i}$	overall speed ratio when the "i" shaft is still
$\tau_{\#o}$	overall speed ratio when the "o" shaft is still
$\tau_{i_{\#o}}$	τ_i when the "o" shaft is still
$\tau_{o_{\#i}}$	τ_o when the "i" shaft is still
$\phi^{z}_{y/x}$	generic three-port differential characteristic function
$\psi^{z}_{y/x}$	fixed-z speed ratio of the planetary gear train in a three port differential
Ψ	basic Willis' ratio
ω_j	angular speed of the jth shaft

Subscripts

m	concurrent with the initial overall speed ratio
M	concurrent with the final overall speed ratio
$\#i$	concurrent with the nodal overall speed ratio $\tau_{\#i}$
#o	concurrent with the nodal overall speed ratio $\tau_{\#o}$

as to explore the other possible equivalent designs by mean of the model presented in [1]. As example, we used it with the GM Voltec multi-mode transmission.

2. Theory

A Power-Split CVT (Fig. 1) consists of a Continuously Variable Unit (CVU) of any kind and of a Power-Split Unit (PSU), which is composed by two (or one) planetary gear trains and up to six fixed-ratio joints (Fig. 2).

Regardless the actual constructive layout, kinematics, power flows and efficiency are ruled by few functional parameters, such as the actual working range of each involved device [1], defined by its initial speed ratio τ_{i_m} τ_{o_m} or τ_m and its ratio spread A_i, A_o or A:

$$A_i = \frac{\tau_{i_M}}{\tau_{i_m}} \qquad A_o = \frac{\tau_{o_M}}{\tau_{o_m}} \qquad A = \frac{\tau_M}{\tau_m} \tag{1}$$

Alternatively, the kinematics may be defined as functions of α_i and α_o. Formerly, α_i and α_o represent the normalized overall transmission ratios for which the input or output shaft of the CVU is null (mechanical points or node points):

$$\alpha_i = \frac{A_i - A}{A_i - 1} = \frac{\tau_{\#i}}{\tau_m} \qquad \alpha_o = \frac{A_o - A}{A_o - 1} = \frac{\tau_{\#o}}{\tau_m} \tag{2}$$

They are related to the ratio spreads, but they may not be actual working points.

However, in an analysis study, the working range of each involved device is not known yet. Accordingly, we have to rearrange the relationships presented in [1] using variables that are independent in respect to the latter.

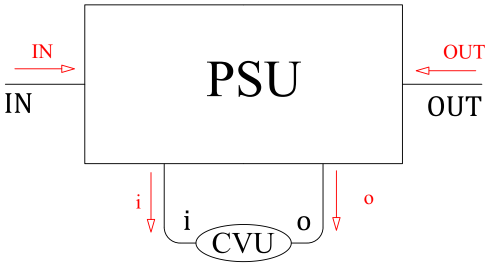

Fig. 1. Basic layout of a power-split CVT, which includes a PSU and a CVU.

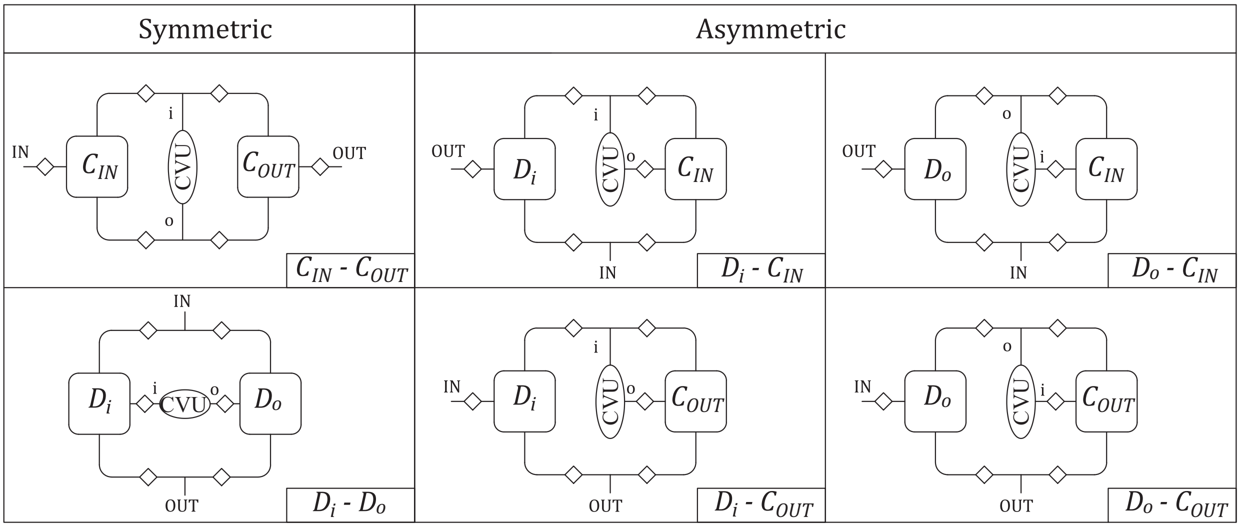

Fig. 2. Functional schemes for compound PS-CVTs. Rhombs represent ordinary gears, while squares represent planetary gear trains.

The ratios τ_i and τ_o are linear functions of τ, so two points are sufficient to define them. Therefore, they can be written also as:

$$\tau_i = \tau_{i_{\#o}} \cdot \frac{\tau - \tau_{\#i}}{\tau_{\#o} - \tau_{\#i}} \qquad \tau = \frac{\tau_i}{\tau_{i_{\#o}}} \cdot (\tau_{\#o} - \tau_{\#i}) + \tau_{\#i} \tag{3}$$

$$\tau_o = \tau_{o_{\#i}} \cdot \frac{\tau - \tau_{\#o}}{\tau_{\#i} - \tau_{\#o}} \qquad \tau = \frac{\tau_o}{\tau_{o_{\#i}}} \cdot (\tau_{\#i} - \tau_{\#o}) + \tau_{\#o} \tag{4}$$

$$\tau_v = \frac{\tau_o}{\tau_i} = -\tau_{v_\#} \cdot \frac{\tau - \tau_{\#o}}{\tau - \tau_{\#i}} \qquad \tau = \frac{\tau_{\#o} + (\tau_v/\tau_{v_\#})\tau_{\#i}}{1 + (\tau_v/\tau_{v_\#})} \qquad \tau_{v_\#} = \frac{\tau_{o_{\#i}}}{\tau_{i_{\#o}}} \tag{5}$$

We selected the present formulation because it has several advantages. It is quite intuitive to identify the overall speed ratios $\tau_{\#i}$ and $\tau_{\#o}$, in correspondence of which one shaft of the CVU is still, as well as the related speed ratios $\tau_{o_{\#i}}$ and $\tau_{i_{\#o}}$. An interesting result is that the ratio $\tau_{v_\#}$ coincides also with the value that τ_v assumes for $\tau = \frac{\tau_{\#i}+\tau_{\#o}}{2}$ and with its opposite for $\tau \to \pm\infty$.

The ideal and real CVU power flow [23], as functions of $\tau_{\#i}$ and $\tau_{\#o}$, become respectively:

$$p_i = \frac{\left(\tau' - \alpha_o\right)\left(\tau' - \alpha_i\right)}{\tau' \ (\alpha_o - \alpha_i)} = \frac{(\tau - \tau_{\#o})(\tau - \tau_{\#i})}{\tau \ (\tau_{\#o} - \tau_{\#i})} \tag{6}$$

$$\overline{p_i} = \frac{\bar{P}_i}{P_{IN}} = \left((1 - \eta_v)\frac{\alpha_o}{\alpha_o - \tau'} + \frac{1}{p_i}\right)^{-1} = \left(\frac{1 - \eta_v}{1 - \tau/\tau_{\#o}} + \frac{1}{p_i}\right)^{-1} \tag{7}$$

$$\eta = 1 - (1 - \eta_v) \ \overline{p_i} \tag{8}$$

Table 1
Funtional groups, involved main shafts and basic characteristic functions.

Group	Shafts	Basic characteristic function
$\boldsymbol{C_{IN}}$	$i,\ o,\ IN$	$\phi_{o/i}^{IN} = \dfrac{1-\tau_{\#i}/\tau}{1-\tau_{\#o}/\tau}$
$\boldsymbol{C_{OUT}}$	$i,\ o,\ OUT$	$\phi_{o/i}^{OUT} = \dfrac{1-(\tau_{\#i}/\tau)^{-1}}{1-(\tau_{\#o}/\tau)^{-1}}$
$\boldsymbol{D_i}$	IN, OUT, i	$\phi_{OUT/IN}^{i} = \tau_{\#i}/\tau$
$\boldsymbol{D_o}$	$IN, OUT,\ o$	$\phi_{OUT/IN}^{o} = \tau_{\#o}/\tau$

All the previous relationships are independent from the actual constructive layout. What is more, $\tau_{\#i}$ and $\tau_{\#o}$ alone govern the characteristic functions, and then the power flow distribution for given scheme [1]. Indeed the PSU is composed by two three-port differentials (i.e. a planetary gearing and up to three fixed-ratio joints). Each three-port differentials can belong to a specific group depending on the involved main shafts (see Table 1) and it is characterized by a specific set of six mutually dependent *characteristic functions*. Table 1 reports the basic ones.

The characteristic functions have a double meaning: $\phi_{y/x}^{z}$ represents $-P_x/P_y$ (the opposite of the ratio between the powers transmitted through two shafts of the three-port differential), but also the possible Willis' ratios providing synchronism [1].

Accordingly, the characteristic functions can be used both for analysis and design purposes. Indeed, only one characteristic function binds the actual Willis' ratio ψ and the synchronous overall transmission ratio τ_* of each planetary gear train, but the others can suggest functionally equivalent alternative solutions (with different teeth ratios and layouts), by mean of the design chart (See Section 5.5).

For example, the planetary gear train PG1 of the D_i three-port mechanism in Section 5 has constructive ratio $\psi = -0.54$ and it is synchronous when the overall transmission ratio is 0.38. Its carrier is linked to the "*OUT*" main shaft, its ring gear is linked to the "*IN*" main shaft and its sun gear is linked to the "*i*" main shaft. Accordingly, it is $\psi = \psi_{ring/sun}^{carr.} = \phi_{IN/i}^{OUT}(0.38) = -0.54$ (See Fig. 9).

Nonetheless, as stated before, $\phi_{IN/i}^{OUT}(\tau)$ represents also the power ratio $-(P_i/P_{IN})|_{D_i}$ in the entire operative range, which means that, for example, known $P_{IN}|_{D_i}$, the other two internal power flows of the D_i three-port mechanism can be easily calculated. Then, as soon as the power flows and speeds external to each three-port mechanism are known, calculating the speed and torques applied directly to the carrier, sun and ring gears is easy, because their speed is just inversely proportional to the value of the fixed gear ratio k_j on the same shaft (see the example in Section 5.1).

3. Direct analysis

In a direct analysis, the known data are:

- Arrangement of the devices within the PSU and their mutual connections;
- Constructive ratios of the involved gear sets (Willis' ratio, teeth ratio between ordinary gear sets etc.);
- Extreme operating conditions of the CVU (i.e. maximum speed and torques of electric or hydraulic machines, extreme speed ratios for mechanical variators etc.).

The objective is to assess the:

- Range of the overall transmission ratio τ;
- Range of transmission ratio τ_i at the input of the CVU;
- Range of transmission ratio τ_o at the output of the CVU;

and thus the functional parameters.

For this purpose, we suggest the following analysis approach:

1 To identify the functional scheme (Fig. 2) and standardize the Willis' ratios (Table 2).
2 To calculate the node points $\tau_{\#i}$ and $\tau_{\#o}$ and the related speed ratios $\tau_{o_{\#i}}$ and $\tau_{i_{\#o}}$ (actual or fictitious, Table 3).
3 To assess the kinematic working ranges bounding the speeds of the CVU.

3.1. Identify the functional scheme

Each functional scheme is a combination of two three-port differentials (a planetary gear train and three ordinary gears) sharing two distinct ports. In order to cover all the possible different constructive solutions of compound or shunt PS-CVTs with the minimum possible number of equations, it is convenient to refer to a standard position for carrier, sun and ring gear of the planetary gear train for each type of three-port differential. If the actual arrangement of the analyzed transmission is different from the standardized one, then the basic Willis' ratio Ψ have to be calculated preventively by mean of the known constructive one. Since it can be a tedious task, we introduced for this purpose a quick look-up table (Table 2):

Table 2
Basic Willis' ratios $\boldsymbol{\Psi}$ as functions of the constructive ones.

Group	$\boldsymbol{\Psi} = \boldsymbol{\psi}^{z}_{y/x}$	$\boldsymbol{\psi}^{z}_{x/y}$	$\boldsymbol{\psi}^{y}_{x/z}$	$\boldsymbol{\psi}^{x}_{y/z}$	$\boldsymbol{\psi}^{x}_{z/y}$	$\boldsymbol{\psi}^{y}_{z/x}$
$\boldsymbol{C_{IN}}$	$\boldsymbol{\psi}^{IN}_{o/i}$	$\dfrac{1}{\psi^{IN}_{i/o}}$	$\dfrac{1}{1-\psi^{o}_{i/IN}}$	$1-\psi^{i}_{o/IN}$	$1-\dfrac{1}{\psi^{i}_{IN/o}}$	$\dfrac{-\psi^{o}_{IN/i}}{1-\psi^{o}_{IN/i}}$
$\boldsymbol{C_{OUT}}$	$\boldsymbol{\psi}^{OUT}_{o/i}$	$\dfrac{1}{\psi^{OUT}_{i/o}}$	$\dfrac{1}{1-\psi^{o}_{i/OUT}}$	$1-\psi^{i}_{o/OUT}$	$1-\dfrac{1}{\psi^{i}_{OUT/o}}$	$\dfrac{-\psi^{o}_{OUT/i}}{1-\psi^{o}_{OUT/i}}$
$\boldsymbol{D_i}$	$\boldsymbol{\psi}^{i}_{OUT/IN}$	$\dfrac{1}{\psi^{i}_{IN/OUT}}$	$\dfrac{1}{1-\psi^{OUT}_{IN/i}}$	$1-\psi^{IN}_{OUT/i}$	$1-\dfrac{1}{\psi^{IN}_{i/OUT}}$	$\dfrac{-\psi^{OUT}_{i/IN}}{1-\psi^{OUT}_{i/IN}}$
$\boldsymbol{D_o}$	$\boldsymbol{\psi}^{o}_{OUT/IN}$	$\dfrac{1}{\psi^{o}_{IN/OUT}}$	$\dfrac{1}{1-\psi^{OUT}_{IN/o}}$	$1-\psi^{IN}_{OUT/o}$	$1-\dfrac{1}{\psi^{IN}_{o/OUT}}$	$\dfrac{-\psi^{OUT}_{o/IN}}{1-\psi^{OUT}_{o/IN}}$

Table 3
Matrices for the calculation of the node points from the constructive data.

Group	$[\boldsymbol{Y_{\#i}}]$		$[\boldsymbol{Y_{\#o}}]$		$\{\boldsymbol{b}\}$
$\boldsymbol{C_{IN}}$	0	$\dfrac{1}{1-\Psi}\cdot\dfrac{k_{IN}}{k_o}$	0	$-\dfrac{\Psi}{1-\Psi}\cdot\dfrac{k_{IN}}{k_i}$	1
$\boldsymbol{C_{OUT}}$	1	$-\dfrac{1}{1-\Psi}\cdot\dfrac{k_{OUT}}{k_o}$	1	$\dfrac{\Psi}{1-\Psi}\cdot\dfrac{k_{OUT}}{k_i}$	0
$\boldsymbol{D_i}$	1	0	1	$-(1-\Psi)\cdot\dfrac{k_{OUT}}{k_i}$	$\Psi\cdot\dfrac{k_{OUT}}{k_{IN}}$
$\boldsymbol{D_o}$	1	$-(1-\Psi)\cdot\dfrac{k_{OUT}}{k_o}$	1	0	$\Psi\cdot\dfrac{k_{OUT}}{k_{IN}}$

3.2. Calculus of the node points

We identify the node points considering that in a three-port differential the speed of each port is a linear function of two others and that the constructive ratio of a simple planetary gear train coincides with the ratio between the ring speed over the sun speed when the carrier is motionless. Therefore, for each group, we can write the following kinematic equations:

$$\boldsymbol{C_{IN}} \qquad 1 = \psi^{o}_{IN/i}\cdot\frac{k_{IN}}{k_i}\cdot\tau_i + \psi^{i}_{IN/o}\cdot\frac{k_{IN}}{k_o}\cdot\tau_o$$

$$\boldsymbol{C_{OUT}} \qquad \tau = \psi^{o}_{OUT/i}\cdot\frac{k_{OUT}}{k_i}\cdot\tau_i + \psi^{i}_{OUT/o}\cdot\frac{k_{OUT}}{k_o}\cdot\tau_o$$

$$\boldsymbol{D_i} \qquad \tau = \psi^{i}_{OUT/IN}\cdot\frac{k_{OUT}}{k_{IN}}\cdot 1 + \psi^{IN}_{OUT/i}\cdot\frac{k_{OUT}}{k_i}\cdot\tau_i$$

$$\boldsymbol{D_o} \qquad \tau = \psi^{o}_{OUT/IN}\cdot\frac{k_{OUT}}{k_{IN}}\cdot 1 + \psi^{IN}_{OUT/o}\cdot\frac{k_{OUT}}{k_o}\cdot\tau_o$$

in which k_j is the fixed ratio between ω_j (external to the three-port mechanism), and the matching speed of the planetary gear train (see Fig. 2).

Detailing the previous equations for the conditions in which either i or o is stopped, and converting, where necessary, the parameters ψ to the basic ones Ψ through the relationships in Table 2, two linear expression for each group are obtained. It is convenient to arrange these equations in two separate systems (see Table 3):

$$[Y_{\#i}]\begin{pmatrix}\tau_{\#i}\\ \tau_{o_{\#i}}\end{pmatrix} = \{b\} \qquad [Y_{\#o}]\begin{pmatrix}\tau_{\#o}\\ \tau_{i_{\#o}}\end{pmatrix} = \{b\} \tag{9}$$

In order to obtain the variables $\tau_{\#i}$, $\tau_{o_{\#i}}$, $\tau_{\#o}$ and $\tau_{i_{\#o}}$ it is sufficient to select from Table 3 only the rows referring to the groups involved in the studied layout, thus obtaining two invertible square sub-matrices of $[Y_{\#i}]$ and $[Y_{\#o}]$ and one 2×1 sub-vector of known terms of $\{b\}$. Clearly, all the involved parameters must refer to their three-port differentials.

In particular, $[Y_{\#i}]$ and $[Y_{\#o}]$ are often triangular, and then the linear system can be solved directly. Only $D_o - C_{OUT}$ and $D_i - C_{OUT}$ can show one full 2×2 matrix. Anyway, for the reader convenience, we reported also the explicit solutions in Tables 6 and 7 of Appendix.

3.3. Kinematic working ranges

By mean of the relationships (3)–(5) it is possible, known one speed ratio among τ, τ_i, τ_o or τ_v, to calculate the remaining ones.

Accordingly, we can obtain the working ranges of the transmission, by imposing the extreme operating conditions of the CVU. Specifically, if the CVU is mechanical, we know τ_{v_m} and τ_{v_M} and we can find the extreme value of τ, by which we can obtain also those of τ_i and τ_o. Similarly, if the CVU is electric or hydraulic, the maximum speed of the "i" and "o" shafts are known, i.e. two of the following four values between τ_{i_m} or τ_{o_m} and τ_{i_M} or τ_{o_M} (see Section 5.1, for an example). Therefore, it is possible to locate the extreme values of τ and, from these, the values of τ_i and τ_o not yet known.

All the functional parameter are now identified and it is possible a thorough use of model [1].

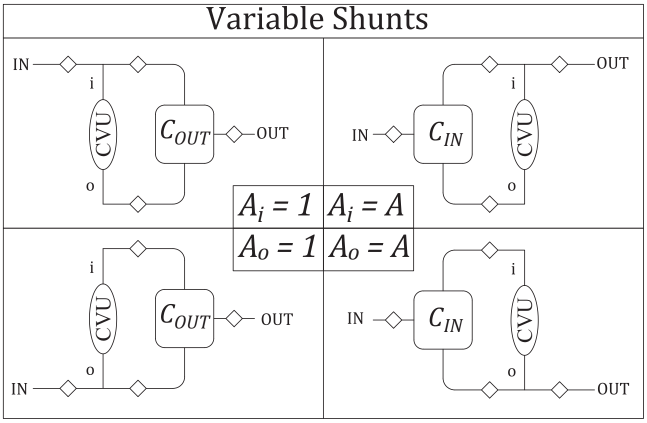

Fig. 3. Shunt transmissions.

Table 4
Fictitious constructive parameters for a Cross Bridge transmission in order to simulate a simple shunt.

Shunt scheme	Cross-Bridge equivalent parameters		
$A_i = 1$	$k_{IN}\|_{C_{IN}} = 1$	$k_i\|_{C_{IN}} = k_{IN}$	$\Psi\|_{C_{IN}} = \psi_{o/i}^{IN} \to \infty$
$A_o = 1$	$k_{IN}\|_{C_{IN}} = 1$	$k_o\|_{C_{IN}} = k_{IN}$	$\Psi\|_{C_{IN}} = \psi_{o/i}^{IN} \to 0$
$A_i = A$	$k_{OUT}\|_{C_{OUT}} = 1$	$k_i\|_{C_{OUT}} = k_{OUT}$	$\Psi\|_{C_{OUT}} = \psi_{o/i}^{OUT} \to \infty$
$A_o = A$	$k_{OUT}\|_{C_{OUT}} = 1$	$k_o\|_{C_{OUT}} = k_{OUT}$	$\Psi\|_{C_{OUT}} = \psi_{o/i}^{OUT} \to 0$

4. Shunt PS-CVTs

The same method may still apply to shunt transmissions, which may be part of multi-mode compound PS-CVTs as well as include only one planetary gear train. This is advantageous because it does not require a separate mathematical model (see the example of Section 5).

4.1. Multimode transmissions

Multimode transmissions usually rely on a system of clutches in order to switch from a compound to a shunt mode and vice-versa. Mathematically, we modeled this operation introducing some fictitious constructive values in the model.

For example, if the mode switch is obtained disconnecting and stopping one shaft of a planetary gear train, then the related value of k would tend to ∞, since the “external” shaft of the three-port mechanism (which is no longer physically connected to the planetary gear train) is free-wheeling, while the internal shaft is stopped.

Similarly, if the switch is obtained by disconnecting one shaft of the planetary gear train and forcing the planet carrier in being synchronous, then we can assume the disconnected shaft as it is the planet carrier of a fictitious planetary gear train with $\psi_{sun2/sun1}^{carr} \to 1$.

This is a kinematic equivalent condition, and then do not modify the power flow distribution. Indeed, the fictitious carrier appears still connected, but it cannot transmit torque and its speed does not influence the other two.

4.2. Simple shunt transmissions

The above procedure and equations result still valid also in the case of simple variable shunt transmissions if we model properly the missing components, i.e.one planetary gearing and two fixed-ratio joints.

For example, an input split transmission with $A_o = A$ (see Fig. 3) is equivalent to as a cross bridge transmission in which it is $k_{OUT}|_{C_{OUT}} = 1$, $k_o|_{C_{OUT}} = k_{OUT}$, $\psi_{o/OUT}^{i} \to 1$, while to establish the value of $k_i|_{C_{OUT}}$ is pointless, since the shaft linked to “i” is no longer able to transmit torque or to effect the other speeds, whichever it is its own speed.

For the reader convenience, in Table 4 we report the fictitious constructive parameters to use in order to deal with any shunt scheme as it were a cross-bridge. However, we want to point out that in order to study a shunt transmission it could be possible using any compound layout as well.

5. Application

In order to explain the method presented above, hereinafter we proceed to the analysis of the GM “Voltec” EV propulsion system, which is the concept of the driveline of the second generation of the Chevrolet Volt. It is an advanced multi-mode transmission, switching between several modes by means of a system of clutches [24–27].

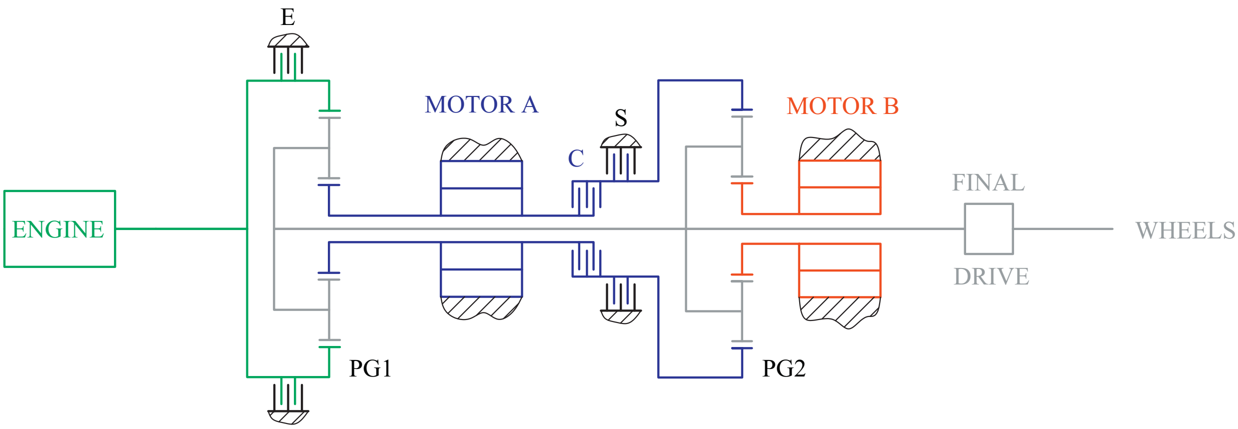

Fig. 4. Simplified constructive layout (derived from the US patent US 6478 705 B1).

Table 5
Different modes obtained by real clutch operations.

Modes	Clutchs		
	E	S	C
FEV, full electric vehicle	Closed	Closed	Open
Shunt PS-CVT, referred as low extended range by GM	Open	Closed	Open
PHEV, fixed-ratio parallel hybrid electric vehicle	Open	Closed	Closed
Compound PS-CVT, referred as high extended range by GM	Open	Open	Closed

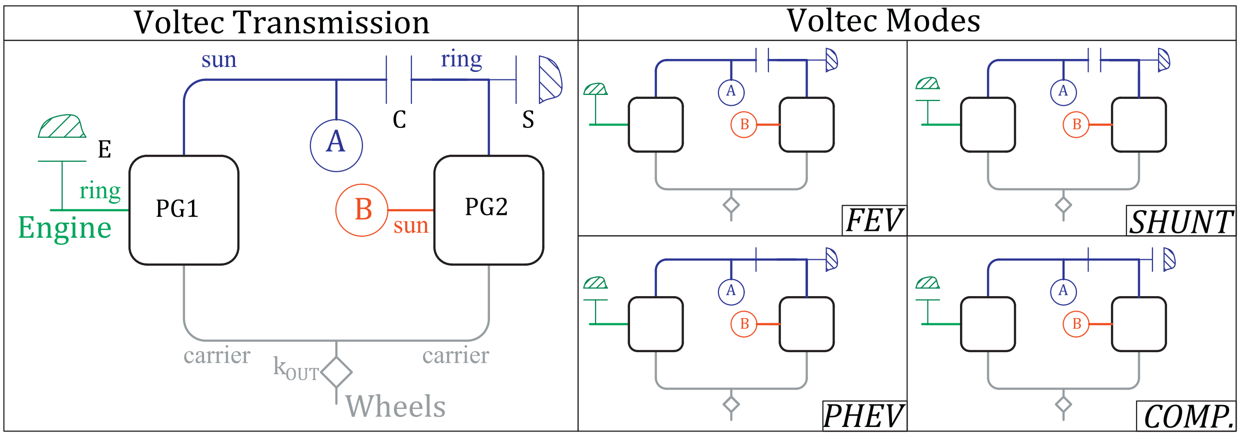

Fig. 5. Constructive scheme and working modes (full electric, parallel hybrid, PS-CVT shunt and compound).

In Fig. 4 we show a simplified equivalent constructive layout, which is derived by a previous patent submitted by the same car manufacturer. We introduced in the sketch also the clutch E in order to model a one-way clutch that prevents the engine from running backwards during full electric operations. The fixed gear ratio of the final drive is obtained thanks to a chain and a planetary reducer.

Table 5 and Fig. 5 summarize the various modes of operations and the corresponding clutches state.

The compound mode and the shunt mode differ for a state change of the clutches C and S. It can be modeled introducing a fictitious ordinary gearing between motor A and the ring gear of PG2, whose gear ratio changes from one to infinite. Therefore, the compound and the shunt mode can share the same mathematical model. Moreover, since the ring gear, which is coupled to the frame during the shunt mode, is motionless also during the compound mode at the node point (when motor A is still), then it is easy to obtain a mode switch without clutch slip in this operating condition.

The parallel mode occurs when both the clutches C and S are closed. This implies that the motor A is still and Motor B only is active as well as during the mode switch between the shunt and the compound. Nevertheless, despite in parallel mode PG1 does not apply torque to motor A but to the frame through clutch C and S, this does not modify the kinematic, and then the power flow distribution. As a result, the parallel hybrid mode can be represented as a particular condition

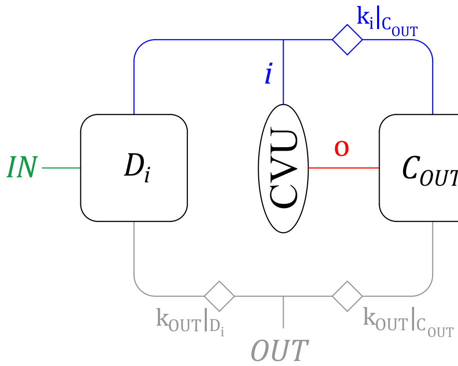

Fig. 6. Functional schematic of the Voltec transmission. The fictitious gear ratio $\boldsymbol{k_i|_{C_{OUT}}}$ models clutches C and S.

either of the shunt PS-CVT, which occurs when clutch S is closed, or of the compound PS-CVT, which occurs when clutch C is closed, and it does not need to be addressed separately.

Eventually, the FEV occurs when both S and E are closed. The ring gear of PG1 linked to the engine is still, so it can be modeled by mean of the shunt PS-CVT working with $\tau \to \infty$. In this case, the system can work either with one or two motors, and their angular speeds are directly proportional to the output speed.

The unified functional scheme can be identified considering that in Fig. 5 motor A, which is one of the CVU shafts, is linked to both the planetary gear trains (PG1 and PG2), while motor B, which represents the other shaft of the CVU, is connected to PG2 only. Accordingly, in Fig. 5 it is represented an asymmetric layout (see Fig. 2). In this case, we can arbitrarily label motor A as the "i" shaft, and then motor B as the "o" shaft of the CVU. In particular, PG2 connects i, o and the output of the whole transmission, and then it belongs to the C_{OUT} group, while PG1 connects i, IN and OUT, and then it belongs to the D_i group. As a result, the scheme is $D_i - C_{OUT}$ (see Fig. 6).

As it can be seen in Fig. 6, we have split the final drive in $k_{OUT} = k_{OUT}|_{D_i} = k_{OUT}|_{C_{OUT}}$ in order to match the basic schemes of Fig. 2 (also the reverse operation is possible when designing the transmission [1]) and we have introduced the fictitious ordinary gearing $k_i|_{C_{OUT}}$ in order to model the operation of clutches C and S.

For the studied transmission it is $\psi_{IN/i}^{OUT} = -0.536$ and $\psi_{i/o}^{OUT} = -0.481$, $k_{OUT}|_{D_i} = k_{OUT}|_{C_{OUT}} = \frac{1}{2.64}$ and $k_i|_{D_i} = k_{IN}|_{D_i} = k_o|_{C_{OUT}} = 1$. Moreover, we assume that the minimum engine speed for a PS-CVT operation is around 1200 rpm, and that the maximum absolute speed for both the electric machines is around 11,000 rpm [24]. Firstly, from Table 2, we obtain that the value of the basic Willis' ratios are $\Psi|_{D_i} = \psi_{OUT/IN}^{i} = 0.652$ and $\Psi|_{C_{OUT}} = \psi_{o/i}^{OUT} = -2.08$. Eventually, for calculation purposes, we replace ∞ with a high finite value, such as 10^{10}.

5.1. Compound mode

The values of the overall transmission ratios $\tau_{\#i}$ and $\tau_{\#o}$, corresponding to the node points, and the related speeds ratios $\tau_{o_{\#i}}$ and $\tau_{i_{\#o}}$, can be calculated through the D_i and C_{OUT} rows of the matrices of Table 3 or the $D_i - C_{OUT}$ rows of Tables 6 and 7 in Appendix. They are $\tau_{\#i} = 0.247$, $\tau_{\#o} = 0.510$, $\tau_{o_{\#i}} = 2.00$ and $\tau_{i_{\#o}} = 2.00$. Instead, the overall transmission ratios corresponding to the synchronous conditions for the two planetary gear trains can be calculated as function of the basic Willis' ratios inverting the basic characteristic functions of Table 1.

$$\tau_*|_{D_i} = \frac{\tau_{\#i}}{\Psi|_{D_i}} = 0.379 \qquad \tau_*|_{C_{OUT}} = \frac{\Psi|_{C_{OUT}} - 1}{\Psi|_{C_{OUT}}/\tau_{\#o} - 1/\tau_{\#i}} = 0.379$$

They coincide because if the homologous ordinary gearing of the two involved groups have the same value (as in our case study) the two PG must have the same synchronous point [1], and it is simply $\tau_* = k_{OUT}/k_{IN}$.

At this point, we can plot $\tau_i(\tau)$ and $\tau_o(\tau)$ by mean of the direct relationships of Eq. (3-5).

The electric motors B and A reach their absolute maximum speed of 11,000 rpm for the speed of the engine at its minimum of 1200 rpm, and so for $|\tau_o| = |\tau_i| = 9.17$; the theoretical working interval ($\tau_m = -0.69$ and $\tau_M = 1.45$) is obtained thanks to the inverse functions (3)–(5) for $\tau_{o_m} = 9.17$ and $\tau_{i_M} = 9.17$ (see Fig. 7). Accordingly, the unknown speed ratios for the CVU shaft can be calculated through the matching direct relationships of (3)–(5) and their value is $\tau_{i_m} = \tau_i(-0.69) = -7.09$ and $\tau_{o_M} = \tau_o(1.45) = -7.14$. The effective functioning range in compound mode is much narrower, because of the presence of the shunt mode, which is preferable for $\tau < \tau_{\#i}$, because of the electronically limited maximum vehicle speed, and because it is not always possible or convenient to operate the engine at its minimum speed. However, for analysis purposes, this does not modify nor invalidate the obtained results.

The internal power flows can be easily assessed thanks to the characteristic functions, which are functions of the basic ones (Table 1). Since the main kinematics are known, calculating also the internal speeds and torques is trivial. For example,

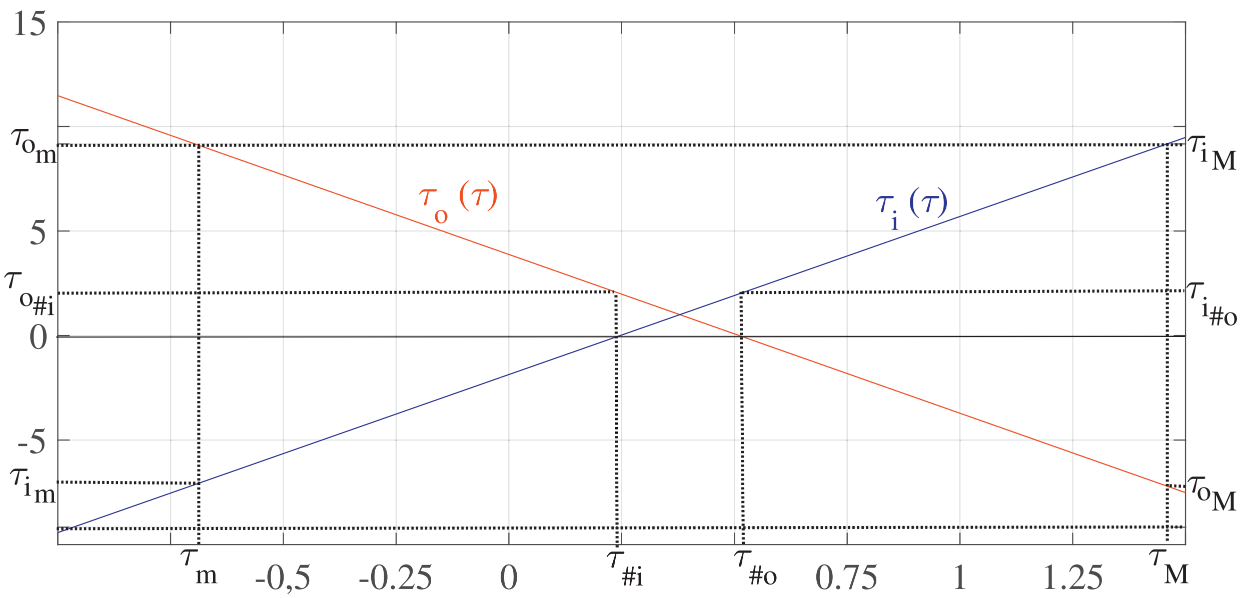

Fig. 7. Compound mode: kinematic relationships and theoretical working range.

for the carrier of the second planetary gear train it is $\overline{p}_{OUT}|_{C_{OUT}} = -\phi^{i}_{o/OUT} \cdot \overline{p}_o|_{C_{OUT}} = -(1-\phi^{OUT}_{o/i}) \cdot \ \eta_v \ \overline{p}_i$, while the absolute speed and torque are $\omega_{carr}|_{C_{OUT}} = \frac{\tau}{k_{OUT}|_{C_{OUT}}} \cdot \ \omega_{IN}$ and $\overline{T}_{carr}|_{C_{OUT}} = \frac{\overline{p}_{OUT}}{\omega_{carr}}|_{C_{OUT}} \cdot \ P_{IN}$ (for a more detailed example, see [1]).

5.2. Mode switch and parallel mode

The mode switch occurs for $\tau_{\#i} = 0.247$, by disengaging the clutch C and engaging S. However, if C is not disengaged, then a fixed-ratio parallel hybrid mode occurs, since the speed of both engine and motor B are not free ($\tau_{o_{\#i}} = 2.00$); nonetheless, motor B can absorb or deliver power provided a proper state of charge of the batteries. This condition can be considered as a particular compound or shunt PS-CVT functioning with $\eta_v \to \pm\infty$.

5.3. Shunt mode

The shunt mathematically differs from the compound only for $k_i|_{C_{OUT}} \to \infty$ (instead of $k_i|_{C_{OUT}} = 1$). As a result, the values of the overall transmission ratios $\tau_{\#i}$ e $\tau_{\#o}$ corresponding to the node points, as well as those of $\tau_{o_{\#i}}$ and $\tau_{i_{\#o}}$, are calculated through the same relationships of the compound mode, just setting $k_i|_{C_{OUT}} = 10^{10}$.

The value of the overall transmission ratios $\tau_{\#i}$ e $\tau_{\#o}$ are $\tau_{\#i} = 0.247$ and $\tau_{\#o} = -0.478 \cdot 10^{-10} \approx 0$, while $\tau_{o_{\#i}} = 2.00$ and $\tau_{i_{\#o}} = -1.87$. The value of the synchronous ratios are $\tau_*|_{D_i} = 0.379$ and $\tau_*|_{C_{OUT}} = 0.707 \cdot 10^{-10} \approx 0$.

In this case, the theoretical working interval ($\tau_m = -0.97$ and $\tau_M = 1.13$) is obtained for $\tau_{i_m} = -9.17$ and $\tau_{o_M} = 9.17$ (see Fig. 8). Accordingly, the unknown speed ratios are $\tau_{i_M} = \tau_i(1.13) = 6.68$ and $\tau_{o_m} = \tau_o(-0.97) = -7.88$. Eventually, also the effective functioning range of the shunt mode is expected to be narrower, because of the presence of the compound mode for $\tau > \tau_{\#i}$ and because of the limited vehicle reverse speed.

5.4. Full electric and cranking of the engine

The FEV mode coincides with the shunt for $\tau \to \infty$. In this case, the speed of the engine is no longer significant, as it musts exist a direct proportionality between ω_i, ω_o and ω_{OUT}. Indeed, introducing this value in the relationships (3)–(5) used before, we obtain $(\omega_i/\omega_{OUT})|_{FEV} = \tau_i(10^{10})/10^{10} = 7.57$ and $(\omega_o/\omega_{OUT})|_{FEV} = \tau_o(10^{10})/10^{10} = 8.12$.

Accordingly, starting the IC engine from its standstill is equivalent to a transitory shunt PS-CVT functioning outside its theoretical working range (see Fig. 8). At first the overall speed ratio τ is infinite, and $\eta(\infty) = -\frac{\overline{P}_{OUT}}{\overline{P}_{IN}}|_{\tau\to\infty} \to -\tau \frac{\eta_v - 1}{\tau_{\#i}}$ and $\overline{\theta}(\infty) = \frac{\overline{T}_{OUT}}{\overline{T}_{IN}}|_{\tau\to\infty} \to \frac{\eta_v - 1}{\tau_{\#i}}$ (see Eq. (7)). Then, as soon as η_v assumes a finite, greater than one, value (motor A is absorbing power), also the engine starts absorbing power and τ rapidly decreases until the engine reaches its minimum active speed, i.e. for a transmission ratio within the active operating range $\tau_m \div \tau_M$. At this point, the engine starts supplying power itself and the transmission can start its normal PS-CVT functioning, progressively modifying the engine speed, overall transmission

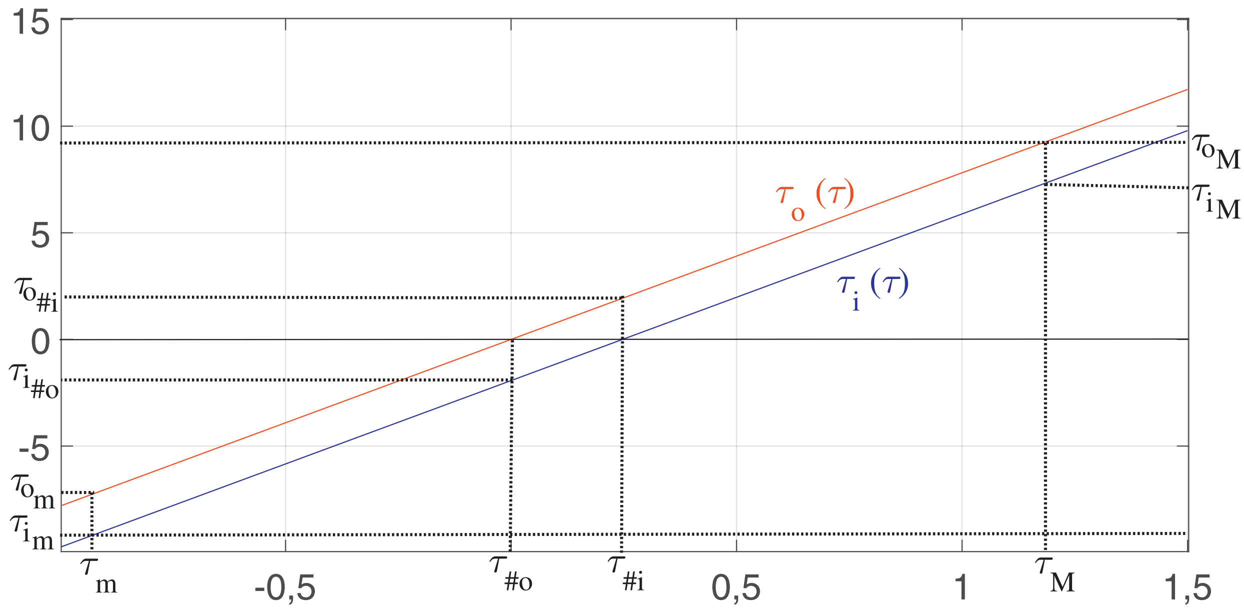

Fig. 8. Shunt mode: kinematic relationships and theoretical working range.

ratio and mode so that the desired performance is achieved. Indeed, the swapping from full electric to hybrid usually occurs at low speeds, but the car, as a FEV, is able to reach the typical speed range of the compound mode.

5.5. Constructive simplification

One of the strengths of the design model [1] is that it suggests possible constructive simplification. In the current case study, the two planetary gear trains have the same synchronous point $\tau_* = k_{OUT} = \frac{1}{2.64} = 0.379$ and very similar Willis' ratios, i.e. $\psi_{IN/i}^{OUT} = -0.536$ and $\psi_{i/o}^{OUT} = -0.481$. Two plausible teeth ratios are $\psi_{IN/i}^{OUT} = -\frac{60}{112}$ and $\psi_{i/o}^{OUT} = -\frac{52}{108}$.

By plotting the design chart [1] (see Fig. 9), it can be seen that it exists a nearby condition which could permit the selection of an alternative design, with two planetary gear trains with the same synchronous point $\tau_* = 0.375$, but also the same gears ($\psi_{IN/i}^{OUT} = \psi_{i/o}^{OUT} = -0.518$), while maintaining the same layout and the same node points, and then the same power flow distribution. For instance, in this case it could be $\psi_{IN/i}^{OUT} = \psi_{i/o}^{OUT} = -\frac{56}{108}$ with $k_{OUT} = \tau_* = 1/2.67$.

This could lead to a slightly more cost-effective transmission, due to the increased economies of scale, while the speed ratio difference for both motor A and B in respect to the original transmission would be within the 5%, whichever the functioning mode. Indeed, the node points are the same, while $\tau_{o_{\#i}} = 1.90$ and $\tau_{i_{\#o}} = 2.06$ are slightly different from the original values ($\tau_{o_{\#i}} = \tau_{i_{\#o}} = 2.00$). Eventually, during FEV functioning both electric motors would spin with the same speed ($\tau_i/\tau = \tau_o/\tau = 7.82$).

6. Results and discussion

The analysis method described in this paper is strictly complementary to the design method [1], and its main scope is the calculation of the functional parameters of existing transmissions. These parameters are important in order to design PS-CVT transmissions, as described in [1]. However, they are important for analysis purposes too, since they consent to obtain in a simple, general and direct way, many other important information, such as speeds, power flows and efficiency (whichever it is the scheme, see Eqs. (3)–(8) and Table 1).

The presented method is immediate (see, for example, Section 5.1), as it requires only to use two simple formulas from Table 2 and to solve two systems of two equations from Table 3 (which is equivalent to the use of four formulas among those listed in Appendix) in order to obtain the main results. Since it aims to generality, it may present more variables than those strictly necessary for a specific case. Nonetheless, these variables are still useful for the analysis of multimode transmissions, and simpler transmissions as well (shunts, discrete). Indeed, this approach consents the use of fictitious constructive ratios, which are intuitive (as they only have to ensure the kinematic equivalence), in order to model complex transmission that may include several functioning modes, without the need to arrange separate systems of equations (see example 5).

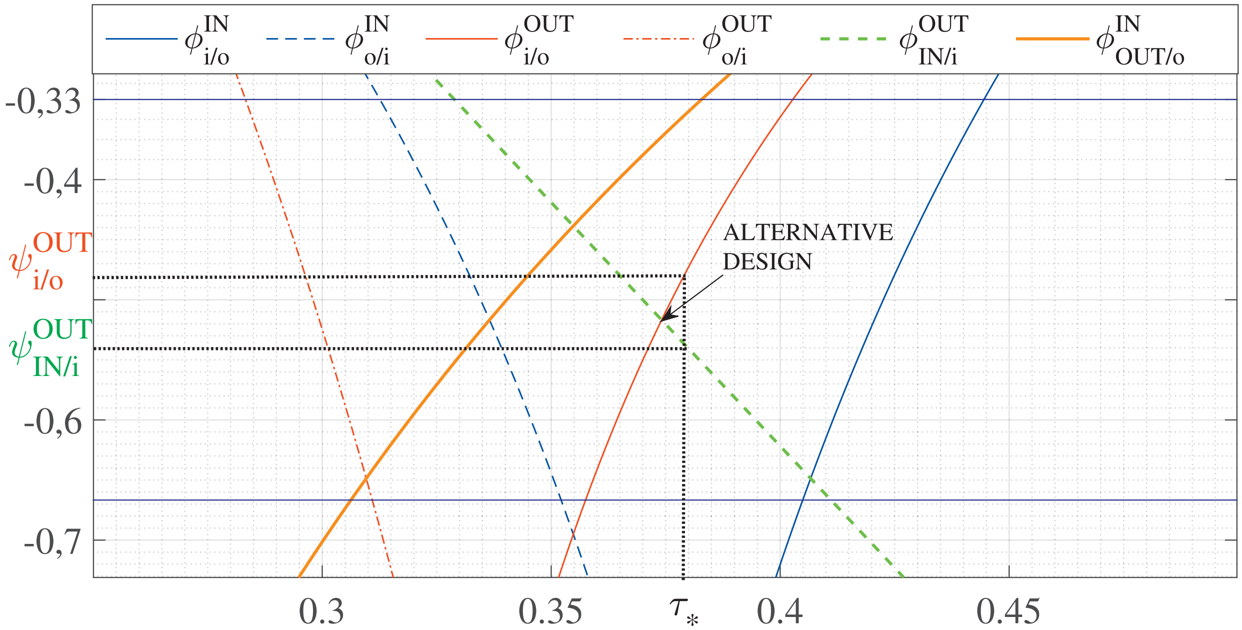

Fig. 9. Design chart for the Voltec transmission ($\tau_{\#i} = 0.247$ and $\tau_{\#o} = 0.510$): current and alternative design.

7. Conclusions

Within this paper, we provide a fast method for the kinematic analysis of compound power-split CVTs, as a counterpart of the design model presented in [1]. Indeed, the analysis of efficiency, power flows and torques, but also the design of functionally equivalent transmissions, can be entirely performed starting from few kinematic parameters. Accordingly, identifying such parameters is useful not only in order to verify a transmission designed with our method [1], but also in order to analyze an existing one.

The approach is general, as it can model compound, shunt or multimode transmissions, whatever the actual constructive scheme. The model has been conceived with numerical implementation in mind, but we have introduced some explicit look-up tables anyway, for disposable calculations. Indeed, since it does not require to be modified for a specific transmission, it greatly reduces the number of equations to be implemented. This consents to avoid the traditional approach, which is often tiresome (many speeds and torques change sign) and can lead to hardly intelligible (and then prone to error) intermediate results, unless the transmission is very simple. Contrariwise, it can be applied easily and rapidly, and it supplies parameters with a simple meaning and multiple uses, eliminating the need to scrutinize large formularies or numerous papers addressing specific cases.

Moreover, thanks to the design chart [1], it is immediate to verify the possibility of realizing a transmission functionally equivalent to an existing one, but with different layout and constructive ratios, or to spot further opportunities of constructive simplification.

Eventually, as an example, we have applied our method to the kinematic analysis of the "Voltec" extended range propulsion system.

Appendix

Table 6
Explicit solutions of the system (9) for the calculation of $\tau_{\#i}$ and $\tau_{o_{\#i}}$.

Scheme	$\tau_{\#i}$	$\tau_{o_{\#i}}$
$C_{IN} - C_{OUT}$	$\tau_{o_{\#i}} \cdot \frac{k_{OUT}}{k_o\ (1-\Psi)}\vert_{C_{OUT}}$	$\frac{k_o\ (1-\Psi)}{k_{IN}}\vert_{C_{IN}}$
$D_i - D_o$	$\frac{k_{OUT}\cdot\Psi}{k_{IN}}\vert_{D_i}$	$\frac{k_o}{1-\Psi}\vert_{D_o} \cdot \left(\frac{\tau_{\#i}}{k_{OUT}} - \frac{\Psi}{k_{IN}}\right)\vert_{D_o}$
$D_i - C_{IN}$	$\frac{k_{OUT}\cdot\Psi}{k_{IN}}\vert_{D_i}$	$\frac{k_o\ (1-\Psi)}{k_{IN}}\vert_{C_{IN}}$
$D_i - C_{OUT}$	$\frac{k_{OUT}\cdot\Psi}{k_{IN}}\vert_{D_i}$	$\tau_{\#i} \cdot \frac{k_o\ (1-\Psi)}{k_{OUT}}\vert_{C_{OUT}}$
$D_o - C_{IN}$	$\tau_{\#o} + \tau_{o_{\#i}} \cdot \frac{k_{OUT}\ (1-\Psi)}{k_o}\vert_{D_o}$	$\frac{k_o\ (1-\Psi)}{k_{IN}}\vert_{C_{IN}}$
$D_o - C_{OUT}$	$\frac{\tau_{\#o}}{1-\frac{k_{OUT}\ (1-\Psi)}{k_o}\vert_{D_o}\cdot\frac{k_o\ (1-\Psi)}{k_{OUT}}\vert_{C_{OUT}}}$	$\tau_{\#i} \cdot \frac{k_o\ (1-\Psi)}{k_{OUT}}\vert_{C_{OUT}}$

Table 7
Explicit solutions of the system (9) for the calculation of $\boldsymbol{\tau_{\#o}}$ and $\boldsymbol{\tau_{i_{\#o}}}$.

Scheme	$\boldsymbol{\tau_{\#o}}$	$\boldsymbol{\tau_{i_{\#o}}}$
$\boldsymbol{C_{IN} - C_{OUT}}$	$-\boldsymbol{\tau_{i_{\#o}}} \cdot \frac{k_{OUT} \cdot \Psi}{k_i\ (1-\Psi)}\lvert_{C_{OUT}}$	$-\ \frac{k_i\ (1-\Psi)}{k_{IN}\ \cdot \Psi}\lvert_{C_{IN}}$
$\boldsymbol{D_i - D_o}$	$\frac{k_{OUT} \cdot \Psi}{k_{IN}}\lvert_{D_o}$	$\frac{k_i}{1-\Psi}\lvert_{D_i} \cdot \left(\frac{\boldsymbol{\tau_{\#o}}}{k_{OUT}} - \frac{\Psi}{k_{IN}}\right)\lvert_{D_i}$
$\boldsymbol{D_i - C_{IN}}$	$\boldsymbol{\tau_{\#i}} + \boldsymbol{\tau_{i_{\#o}}} \cdot \frac{k_{OUT}\ (1-\Psi)}{k_i}\lvert_{D_i}$	$-\ \frac{k_i\ (1-\Psi)}{k_{IN}\ \cdot \Psi}\lvert_{C_{IN}}$
$\boldsymbol{D_i - C_{OUT}}$	$\frac{\boldsymbol{\tau_{\#i}}}{1 + \frac{k_{OUT}\ (1-\Psi)}{k_i}\lvert_{D_i} \cdot \frac{k_i\ (1-\Psi)}{k_{OUT}\ \cdot \Psi}\lvert_{C_{OUT}}}$	$-\ \boldsymbol{\tau_{\#o}} \cdot \frac{k_i\ (1-\Psi)}{k_{OUT}\ \cdot \Psi}\lvert_{C_{OUT}}$
$\boldsymbol{D_o - C_{IN}}$	$\frac{k_{OUT} \cdot \Psi}{k_{IN}}\lvert_{D_o}$	$-\ \frac{k_i\ (1-\Psi)}{k_{IN}\ \cdot \Psi}\lvert_{C_{IN}}$
$\boldsymbol{D_o - C_{OUT}}$	$\frac{k_{OUT} \cdot \Psi}{k_{IN}}\lvert_{D_o}$	$-\ \boldsymbol{\tau_{\#o}} \cdot \frac{k_i\ (1-\Psi)}{k_{OUT}\ \cdot \Psi}\lvert_{C_{OUT}}$

References

[1] M. Cammalleri, D. Rotella, Functional design of power-split CVTs: an uncoupled hierarchical optimized model, Mech. Mach. Theory 116 (2017) 294–309.
[2] H. Naunheimer, B. Bertsche, J. Ryborz, W. Novak, Automotive Transmissions: Fundamentals, Selection, Design and Application, Springer-Verlag, Berlin, 2011.
[3] L. Guzzella, A. Sciarretta, Vehicle propulsion systeme propulsion systems, Introduction to Modelling and Optimization, Springer-Verlag, Berlin, 2013.
[4] R. Fischer, F. Küçükay, G. Jürgens, R. Najork, B. Pollak, The Automotive Transmission Book, Springer International Publishing, Switzerland, 2015.
[5] D.J. Sanger, The determination of power flow in multiple-path transmission systems, Mech. Mach. Theory 7 (1972) 103–109.
[6] A. Villeneuve, Dual mode electric infinitely variable transmission, SAE Technical Paper 2004-40-0019 (2004).
[7] A. Beccari, M. Cammalleri, F. Sorge, Experimental Results for a Two-Mode Split-Way CVT, VDI Berichte 1709 (2002) 237–250.
[8] B. Conlon, Comparative analysis of single and combined hybrid electrically variable transmission operating modes, SAE World Congr 2005 (2005).
[9] J.M. Miller, Hybrid electric vehicle propulsion system architectures of the e-CVT type, IEEE Trans. Power Electron. 21 (2006) 756–767.
[10] P. Mattsson, Continuously Variable Split-Power Transmission with Several Modes, Chalmers University of Technology, Göteborg, Sweden, 1996 ISBN 91-7197-356-7.
[11] G. Mantriota, Performances of a series infinitely variable transmission with type I power flow, Mech. Mach. Theory 37 (2002) 555–578.
[12] G. Mantriota, Performances of a parallel infinitely variable transmission with a type II power flow, Mech. Mach. Theory 37 (2002) 579–597.
[13] F. Bottiglione, G. Mantriota, MG-IVT: an infinitely variable transmission with optimal power flows, ASME J. Mech. Des. 130 (11) (2008).
[14] K. Pettersson, K.E. Rydberg, P. Krus, Comparative study of multiple mode power split transmissions for wheel loaders, 12th Scand. Int. Conf. Fluid Power (SICFP2011), 2011 May 18–20.
[15] M. Cammalleri, A new approach to the design of a speed-torque-controlled rubber V-belt variator, Proc. Inst. Mech. Eng. Part D 219 (2005) 1413–1427.
[16] E. Pennestrì, L. Mariti, P.P. Valentini, V.H. Mucino, Efficiency evaluation of gearboxes for parallel hybrid vehicles: theory and applications, Mech. Mach. Theory. 49 (2012) 157–176.
[17] J.R. Gomà Ayats, U. Diego-Ayala, J. Minguella Canela, F. Fenollosa, J. Vivancos, Hypergraphs for the analysis of complex mechanisms comprising planetary gear trains and other variable or fixed transmissions, Mech. Mach. Theory 51 (2012) 217–229.
[18] A.K. Gupta, C.P. Ramanarayanan, Analysis of circulating power within hybrid electric vehicle transmissions, Mech. Mach. Theory 64 (2013) 131–143.
[19] M. Cammalleri, F. Sorge, Approximate closed-form solutions for the shift mechanics of rubber belt variators, Proceeding of ASME (IDETC 2009), August 30 - September 2, 2009, doi:10.1115/DETC2009-86638.
[20] F. Bottiglione, S. De Pinto, G. Mantriota, Infinitely variable transmissions in neutral gear: torque ratio and power re-circulation, Mech. Mach. Theory 74 (2014) 285–298.
[21] W. Wang, R. Song, M. Guo, S. Liu, Analysis on compound-split configuration of power-split hybrid electric vehicle, Mech. Mach. Theory 78 (2014) 272–288.
[22] F. Yang, J. Feng, H. Zhang, Power flow and efficiency analysis of multi-flow planetary gear trains, Mech. Mach. Theory 92 (2015) 86–99.
[23] M. Cammalleri, Efficiency of split-way CVT ' s. a simplified model, SAE Technical Paper 2007-24-0133 (2007), doi:10.4271/2007-24-0133.
[24] Conlon, The next generation “Voltec” extended range ev propulsion system, SAE Int. J. Alt. Power 4 (July (2)) (2015), doi:10.4271/2015-01-1152.
[25] A.G. Holmes, M.R. Schmidt, Hybrid electric powertrain including a two-mode electrically variable transmission. US Patent 6 478 705 B1, 2002.
[26] B.M. Conlon, R. Hills, K.M. Rahman, T.J. Blohm, S. Jurkovic, Multimode electrically variable transmission having a ferrite magnet motor and method of operating the same. US Patent US 8 602 938 B1, 2013.
[27] X. Zhang, S.E. Li, H. Peng, J. Sun, Design of multimode power-split hybrid vehicles - a case study on the voltec powertrain system, IEEE Trans. Veh. Technol. 65 (2016) 4790–4801.